Science of the Total Environment 658 (2019) 753–762

Contents lists available at ScienceDirect

Science of the Total Environment

journal homepage: www.elsevier.com/locate/scitotenv

Evaluating the influence of climate change on the fate and transport of fecal coliform bacteria using the modified SWAT model

Dong Jin Jeon [a], Mayzonee Ligaray [b], Minjeong Kim [b], Gayoung Kim [b], Gil Lee [b], Yakov A. Pachepsky [a], Dong-Hyun Cha [b,*], Kyung Hwa Cho [b,*]

[a] USDA-ARS, Environmental Microbial and Food Safety Laboratory, 10300 Baltimore Avenue, Building 173, BARC-East, Beltsville, MD, 20705, USA
[b] School of Urban and Environmental Engineering, Ulsan National Institute of Science and Technology, Ulsan 44919, Republic of Korea

HIGHLIGHTS

- The modified bacteria module successfully predicted fecal coliform bacteria in water.
- Temperature was the dominant control for the fecal coliform population in soil.
- Precipitation was the dominant control for the fecal coliform transport to water bodies.
- Monitoring streambed bacteria is critical for the water quality projections.

GRAPHICAL ABSTRACT

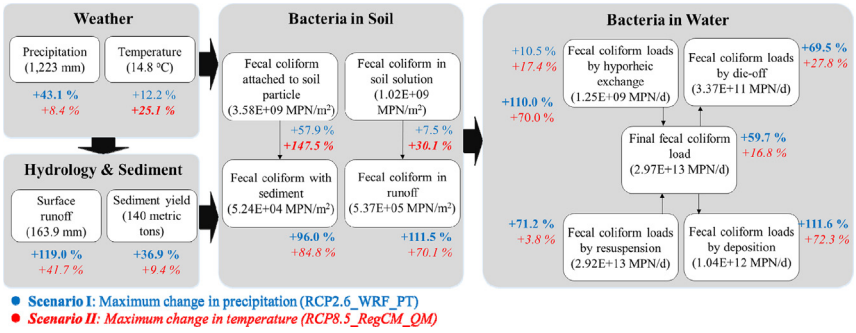

ARTICLE INFO

Article history:
Received 18 October 2018
Received in revised form 12 December 2018
Accepted 13 December 2018
Available online 14 December 2018

Editor: Ashantha Goonetilleke

Keywords:
Climate change
Fecal coliform bacteria
Soil and water assessment tool
Fate and transport

ABSTRACT

Fecal coliform bacteria (FCB) contamination of natural waters is a serious public health issue. Therefore, understanding and anticipating the fate and transport of FCB are important for reducing the risk of contracting diseases. The objective of this study was to analyze the impacts of climate change on the fate and transport of FCB. We modified both the soil and the in-stream bacteria modules in the soil and water assessment tool (SWAT) model and verified the prediction accuracy of seasonal variability of FCB loads using observations. Forty bias-correcting GCM-RCM projections were applied in the modified SWAT model to examine various future climate conditions at the end of this century (2076–2100). Lastly, we also compared the variability of FCB loads under current and future weather conditions using multi-model ensemble simulations (MMES). The modified SWAT model yielded a satisfactory performance with regard to the seasonal variability of FCB amounts in the soil and FCB loading to water bodies. The modified SWAT model presented substantial proliferation of FCB in the soil (30.1%–147.5%) due to an increase in temperature (25.1%). Also, increase in precipitation (53.3%) led to an increase in FCB loads (96.0%–115.5%) from the soil to water body. In the in-stream environment, resuspension from the stream bed was the dominant process affecting the amount of FCB in stream. Therefore, the final FCB loads increased by 71.2% because of the growing peak channel velocity and volume of water used due to an increase in precipitation. Based on the results of MMES, we concluded that the level of FCB would increase simultaneously in the soil as well as in stream by the end of this century. This study will aid in understanding the future variability of FCB loads as well as in preparing an effective management plan for FCB levels in natural waters.

© 2018 Elsevier B.V. All rights reserved.

* Corresponding authors.
E-mail addresses: dhcha@unist.ac.kr (D.-H. Cha), khcho@unist.ac.kr (K.H. Cho).

https://doi.org/10.1016/j.scitotenv.2018.12.213
0048-9697/© 2018 Elsevier B.V. All rights reserved.

1. Introduction

Fecal coliforms are a group of bacteria found in the fecal material of humans and warm-blooded animals (Hagedorn et al. 1999). These bacteria can enter water bodies through various routes such as agricultural runoff, human sewage, wild and domestic animal feces, and re-suspension from streambeds (Baxter-Potter and Gilliland 1988; Graczyk et al. 2010; Scott et al. 2002). Fecal contamination of water body is a serious public health issue because of potential for disease development (Lipp et al. 2001). Therefore, it is critical to assess the fecal coliform population for current management and long term projections of public health.

Meteorological conditions (e.g., precipitation, temperature, and solar intensity) are well known as major factors affecting the fate and transport of fecal coliforms (Cho et al. 2016a; Hong et al. 2010; St Laurent and Mazumder 2014). Precipitation tends to have a positive relationship with the level of fecal coliforms in the soil and in stream (Kistemann et al. 2002). In the soil, survival of *E. coli* was positively associated with soil moisture (Guan and Holley 2003). Cha et al. (2010) concluded that rainfall intensity strongly affects fecal coliform concentration in water body because of the first flush of pollution coming with runoff. Cho et al. (2010) also established that resuspension from the sediment bed dominantly contributed to a boost in fecal coliform concentration in an aquatic environment during rainfall events. In addition, many researchers have explored the relationship between temperature and fecal coliform concentrations. Sinton et al. (2007) observed proliferation of *E. coli* and fecal streptococci in spring, summer, and autumn when the water content of cow pats was >80%. Noor et al. (2013) conducted a spot test and found that the normal growth temperatures of *E. coli* were between 25 °C to 30 °C, with a maximum growth rate at 37 °C. In water bodies, the growth rates of *E. coli* increase with increasing temperature (Hendricks 1972). Also, solar radiation is considered an important factor for the survival of fecal coliform in water bodies (Sinton et al. 2002; Whitman et al. 2004; Cho et al. 2016b). Overall, according to previous studies, populations of fecal coliform bacteria (FCB) are very sensitive to meteorological conditions. Therefore, it is worthwhile to explore the variability of FCB under different climate scenarios.

Climate change is already driving a rise in global mean temperature (Alexander et al. 2006). Several climate models have indicated that a higher temperature will increase the rate of evapotranspiration, thereby increasing precipitation intensity (Meehl et al. 2005; Schär et al. 1999; Trenberth 2011; Wentz et al. 2007). Consequently, climate change can lead to serious threats to public health. Since fecal coliforms are considered to be indicators of microbial water quality, it is important to assess changes variation in fecal coliform concentrations. Since these concentrations tend to be related to precipitation and temperature (St Laurent and Mazumder 2014), climate change scenarios are useful for anticipating the impact of climate change on variability in fecal coliform concentrations. Currently climate change scenarios offer drastically dissimilar predictions depending upon different approaches (e.g., representative concentration pathways, regional climate models, and bias correction methods) (Baek et al. 2013a; Lee et al. 2014; Teutschbein and Seibert 2012). Therefore, prediction of future level of FCB should be evaluated with consideration for the uncertainty of climate change.

Modeling approaches are useful to better understand the fate and transport of FCB. Models can also quantitatively estimate the variability of loads and concentrations of FCB from the soil surface to the receiving stream in accordance with changing environmental conditions (Benham et al. 2006; Cho et al. 2016a; Hofstra 2011; Jamieson et al. 2004). Baffaut and Sadeghi (2010) concluded that the bacteria module of the Soil and Water Assessment Tool (SWAT) reasonably simulated the range and frequencies of bacteria concentrations. However, this model did not incorporate the effects of temperature and other in-stream processes. Thus, Cho et al. (2016a) added a temperature criterion for the growth rate of FCB and verified the improvement of the prediction accuracy. Kim et al. (2017) also devised a new SWAT bacteria module for tropical regions. However, the impacts of climate change on FCB based on modified bacteria modules remains to be evaluated.

This study investigated the variability of FCB at the soil surface and in water bodies under several climate change scenarios. We coupled the new SWAT bacteria module by Kim et al. (2017) with the soil bacteria module developed by Cho et al. (2016a). The objectives of this study were: (1) to explore the changes of climate conditions in the late 21st century by considering various climate change scenarios; (2) to verify the relationship between meteorological factors (e.g., precipitation and temperature) and variability of FCB from the soil surface to receiving streams; and, (3) to predict the level of FCB under future climate conditions using multi-model ensemble simulations.

2. Methods

2.1. Study structure

Fig. 1 shows the structure of this study, which is classified in three parts. The first step was to modify both the soil and in-stream bacteria modules of the SWAT model for FCB load simulations. The model was calibrated using observation data from 2007 to 2016. In Step 2, 40 climate change scenarios (2076–2100) from four representative concentration pathways (RCPs) of the global climate model (GCM), five different regional climate models (RCMs), and two bias correction methods were prepared. The impacts of the climate change scenarios were then analyzed and quantified in Step 3 by integrating the SWAT model built in Step 1 using the weather data from Step 2. The multi-model ensemble simulations were then applied to estimate future FCB loads.

2.2. Study area

The Taehwa River Watershed (TRW) was selected for this study. The Taehwa River (TR) has a length of 47.54 km and flows towards the East Sea by passing through Ulsan City (UC), a metropolitan city located at the southeast of the Korean Peninsula. The TRW was delineated to have the Samho station as an outlet for the area upstream; it covered the area of about 417.6 km^2. Forest covered 70% of the watershed, 16% and 6% were in rice and potato area, and urbanized area covered 5% (Fig. S1). The manure fertilizer was applied in May for rice area and in Mar and Aug for potato area. The regional climate is of the Asian monsoon type with hot and rainy summer and cold and dry winter (Ligaray et al. 2016). The historical annual mean temperature and precipitation are 14.1 °C and 1277 mm, respectively, for a 30-year period (1981 to 2010) at the Ulsan weather station in UC.

2.3. SWAT model description

The SWAT model, developed by the United States Department of Agriculture, is a physical-based semi-distributed model (Arnold et al. 1998). It simulates stream flow and nutrient loads over prolonged periods, and is applicable in evaluating the impacts of environmental change such as land-use and climate on hydrology and nutrient loads in watersheds (Li et al. 2009). A watershed of SWAT model is discretized into sub-basins using topographical data. The sub-basins are split into hydrologic response units (HRUs) that are characterized by dominant land use, soil type, and slope (Gitau et al. 2004).

2.4. Bacteria module modification

The SWAT source code of both the soil and in-stream bacteria modules was modified to improve the prediction accuracy. The original soil bacteria module of SWAT model dealt only with the single value of the

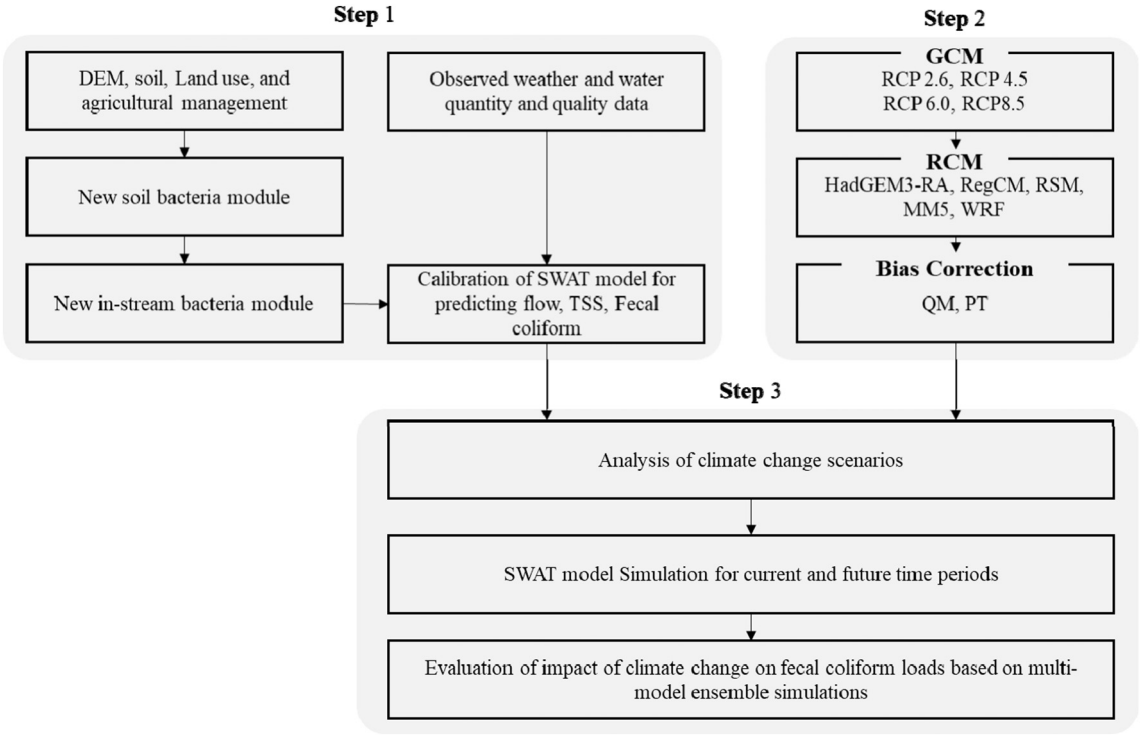
Step 1
DEM, soil, Land use, and agricultural management
Observed weather and water quantity and quality data
New soil bacteria module
New in-stream bacteria module
Calibration of SWAT model for predicting flow, TSS, Fecal coliform
Step 2
GCM
RCP 2.6, RCP 4.5
RCP 6.0, RCP8.5
RCM
HadGEM3-RA, RegCM, RSM, MM5, WRF
Bias Correction
QM, PT
Step 3
Analysis of climate change scenarios
SWAT model Simulation for current and future time periods
Evaluation of impact of climate change on fecal coliform loads based on multi-model ensemble simulations

Fig. 1. Diagram of the fate and transport analysis for fecal coliform bacteria under various future climate conditions based on the modified bacteria module in the SWAT model. DEM -digital elevation model, TSS – total suspended solids, GCM – global circulation model, RCM – regional circulation model, QM – quantile mapping, and PT – power transformation.

media-specific constant rate for re-growth and die-off of bacteria. Therefore, it did not reproduce the seasonal variation of bacteria depending on soil temperature, as follows:

$$bact_{media,i} = bact_{media,i-1} \times \exp(\mu_{net}) - bact_{min} \quad (1)$$

$$\mu_{net,20} = \mu_{die,20} - \mu_{grw,20} \quad (2)$$

where, $bact_{media,i}$ and $bact_{media,i-1}$ are the amount of FCB present in three media types (i.e., foliage, soil solution, and sorbed to the soil) on day i and $i-1$ (MPN/m^2), μ_{net} is the overall rate constant for die-off/re-growth of FCB (1/day), $bact_{min}$ is the minimum daily loss of FCB (MPN/m^2), and $\mu_{die,20}$ and $\mu_{grw,20}$ are the rate constants for die-off and growth of FCB at 20 °C (1/day), respectively.

Cho et al. (2016a) complemented this module by adding an air temperature criterion that determines whether re-growth or die-off should be used in the daily simulations. The number of FCB present in all three media increases when the air temperature is greater than the temperature threshold, whereas the number of FCB decreases when the air temperature is lower than the threshold.

$$bact_i = \begin{cases} bact_{i-1} \times \exp\left(\mu_{grw,20}\right) - bact_{min}, \text{ if } T_{air} \geq T_c \\ bact_{i-1} \times \exp\left(\mu_{die,20}\right) - bact_{min}, \text{ if } T_{air} < T_c \end{cases} \quad (3)$$

where T_{air} is the air temperature and T_c is the temperature threshold.

In the in-stream bacteria module, the original SWAT model considers the number of bacteria settled from the water body and released from the streambed in calculating the amount of bacteria in the water body. However, this version could not correctly simulate bacteria numbers during the dry season (Kim et al. 2017). Park et al. (2017) demonstrated that the bacteria concentration in low-flow conditions is dependent on hyporheic exchange. Kim et al. (2017) also showed that the prediction accuracy of bacteria concentration could be improved when the hyporheic exchange term is added in the original model during the dry season. This study applied the following equations:

$$bact_{water} = bact_{water,i} + bact_{release} + bact_{hyporheic} - bact_{settle} \quad (4)$$

where $bact_{water}$ is the number of FCB in the water body (MPN), $bact_{water,i}$ is the number of FCB in the water body since time began (MPN), $bact_{release}$ is the number of FCB released from the streambed (MPN), $bact_{hyporheic}$ is the number of FCB released by hyporheic exchange into the water body (MPN), and $bact_{settle}$ is the number of FCB settled from water body.

Eqs. (5) and (6) define the hyporheic exchange in the modified bacteria module, wherein $bact_{hyporheic}$ was calculated by (Grant et al. 2011):

$$bact_{hyporheic} = conc_{pore} \times Q_h \quad (5)$$

$$conc_{pore} = conc_{bact,sed} \times \frac{\rho_b}{\varnothing} \quad (6)$$

where $conc_{pore}$ is the FCB concentration in the pore fluid (MPN/m^3), Q_h is the rate of water going to the stream by moving through the pores via hyporheic exchange (−), $conc_{bact,sed}$ is the FCB concentration in the stream bed (MPN/ton sediment in stream bed), ρ_b is the bulk density of the stream bed (g/cm^3), and $\varnothing$ is the bed porosity (−).

2.5. SWAT model setup

ArcSWAT (version 2012.10_2.16) for ArcGIS platform 10.2.2 was used. The SWAT model requires several types of information (i.e., meteorological, geological, and hydrologic data). The details of data acquisition are shown in section S1 in supplemental information. The watershed delineation produced 19 sub-basins and 125 HRUs. The simulation period of 12 years from January 2005 to December 2016 was set up for the watershed (spin-up period: 2005–2006, calibration period: 2007–2016). We adopted the Hargreaves method for calculating potential evapotranspiration. This method considers the temporal

variation of temperature and precipitation (Hargreaves et al. 1985). After the boundary conditions of the SWAT model were established, sensitivity analysis and calibration of the daily flow and monthly sediment loads were performed using Sequential Uncertainty Fitting version-2 (SUFI-2) in the SWAT calibration and uncertainty procedure (SWAT-CUP). For the monthly FCB load prediction, the sensitivity analysis and calibration for examining the new parameters in the updated bacteria module were respectively carried out by Latin Hypercube-One Factor at a Time (LH-OAT) and the pattern search algorithm in MATLAB (Jeon et al. 2018). The correlation coefficient (R^2) and Nash-Sutcliffe model efficiency (NSE) were used for model performance evaluation with regards to flow, sediment load, and FCB load prediction.

2.6. Climate change scenarios

Five Regional Climate Models (RCMs) (i.e., HadGEM3-RA, RegCM4, MM5, WRF, and GRIMs), employed in the Coordinated Regional Climate Downscaling Experiment (CORDEX)-East Asia, are used to provide climate change scenarios for South Korea. Five RCMs have different configurations in term of dynamical core, physical parameterization schemes, and vertical coordination. The model configurations of the five RCMs are described in Table S1. Two RCMs (RegCM4 and GRIMs) use hydrostatic dynamical cores, whereas the others (HadGEM3-RA, MM5, and WRF) are based on non-hydrostatic cores. For the recent past, historical simulation with natural and anthropogenic forcings are conducted over the period of 25 years (1981–2005). Four RCP simulations are performed based on the Representative Concentration Pathway (RCP) 2.6/4.5/6.0/8.5 scenarios for the future projection. The details of the RCP scenarios are shown in Section S2. For the consistency of future climate and present climate analysis periods, the RCP simulations were also run for 25 years in the end 21st century (2076–2100). The model domain of all the simulations covers 28°–46° N and 116°–139° E, which includes South Korea (Fig. S1). The output of a HadGEM2-AO simulated by the Korea Meteorological Administration (KMA) is employed for lateral boundary conditions since it exhibits reasonable performance over the East Asian region, as indicated by Baek et al. (2013b). The HadGEM2-AO comprises an atmospheric model with 38 vertical layers (an atmospheric top at about 40 km) and 1.875° × 1.25° horizontal resolution and an oceanic model with 40 vertical layers and 1° horizontal resolution (Martin et al. 2011).

We converted simulated daily near-surface temperature and precipitation data to Automated Surface Observing System (ASOS) station at Ulsan, South Korea (35.56° N, 129.32° E) using bilinear interpolation. Also, we adjusted climate change scenario data by bias correction using power transformation (PT) and quantile mapping (QM) (the same as distribution mapping). PT uses an exponential form to accurately adjust the variance statistics of climate change scenario data (Teutschbein and Seibert 2012). The idea of QM is to adjust the cumulative distribution function of RCM-simulated climate to that of observed climate. ASOS data at Ulsan station were used for the historical period (1981–2005) as observation data.

2.7. Ensemble construction

To estimate a representative fecal coliform response to future climate change, we used the multi-model ensemble simulations (MMES) with the SWAT model by using the daily precipitation and daily maximum and minimum temperatures from 10 climate change scenarios, which were composed by the five RCMs and two bias correction. The climate change scenarios applied in MMES were chosen prior to the simulations. Among the four RCP scenarios, RCP2.6 was selected on the assumption that the Paris Climate Agreement targets will be met. The Agreement assumes that an increase of 1.5 °C in the global surface temperature will be expected by the end of this century, relative to the 1850–1900 period (Jones et al. 2018). To produce outcomes that reflect future climate conditions, MMES were operated using ten RCP2.6 scenarios generated from five RCMs and two bias correction methods.

3. Results and discussion

3.1. SWAT model performance

The SWAT model prediction accuracy was evaluated in terms of daily flow, monthly sediment loads, and monthly FCB loads at Samho Station of the TRW (Fig. S1). Before examining the performance of the SWAT model through calibration, we identified the critical input parameters by performing sensitivity analyses. Table 1 lists the results of the sensitivity analysis and the calibrated values of critical input parameters. The sensitivity analysis tools in SWAT-CUP software identified 10, 7, and 6 parameters among 22, 8, and 24 parameters governing flow, sediments loads, and FCB loads, respectively. After the sensitive parameters were identified, their values were calibrated while retaining the default model values of other parameters during the calibration process. Flow was substantially sensitive to the baseflow recession constant (Alpha_bf), Manning's coefficient (Ch_n2), the Soil Conservation Service (SCS) runoff curve number (Cn2), effective hydraulic conductivity (Ch_k2), deep aquifer percolation fraction (Rchrg_dp), and available water capacity of the soil (sol_awc). Sediment loads were substantially sensitive to the coefficient in the sediment transport equation (Spcon), the peak rate adjustment factor (prf_bsn), and the channel bank erodibility factor (Ch_cov1). Finally, FCB loads were substantially sensitive to regression coefficients in the streambed bacteria concentration equation (Bsc1 and Bsc2), the growth factor (Wgps), and the die-off factor (Wdps) for persistent bacteria adsorbed to soil particles. Sensitivity ranks of the above parameters are listed in Table 1.

Fig. S2 shows the time series plots of observed rainfall as well as the observed and simulated flow, sediment loads, and FCB loads from 2007 to 2016. We observed the seasonal variation in stream flow, sediment loads and FCB loads caused by summer monsoon. These observations showed high flow discharge and high sediment and FCB loads along with hot and rainy weather during summer season (July to September). From Fig. S2(b), the R^2 and NSE values were 0.80 and 0.62, respectively, for the flow rate. These results indicate that the simulated daily flow has satisfactory agreement with the observations during the calibration period according the watershed-scale model evaluation guidelines given by Moriasi et al. (2007). Fig. S2(c) shows the observed and simulated monthly sediment loads with R^2 and NSE values of 0.86 and 0.72, respectively. Based on the Moriasi et al. (2007) guidelines, the SWAT model of sediment loads was considered “good” in terms of the trends and magnitude. This can be observed in Fig. S2(c) that the model satisfactorily predicted the sediment loads during the wet seasons. The monthly FCB loads simulated by the modified SWAT model are shown in Fig. S2(d). The model well reproduced the seasonal variations and observed monthly loads during baseflow, resulting in R^2 and NSE values of 0.84 and 0.55, respectively.

3.2. Projections of climate change

Monthly precipitation at Ulsan is shown according to the RCP scenarios are shown in Fig. S3. A model ensemble for each RCP scenario is calculated with 10 results from five RCMs and two bias correction methods. In observation for 25 years (1981–2005), most precipitation occurs during the summer season, especially in August, under the influences of the East Asian Summer Monsoon and typhoons. Precipitation rapidly increases from May to June and abruptly decreases from August to October. In the historical simulation for 25 years (1981–2005), monthly precipitation is both similar to those in observations because the bias of model output is reduced by bias correction methods (i.e., power transformation and quantile mapping). However, the precipitation amount in August is still underestimated by about 15%. This feature can be associated with the decreased typhoon activity during August indicated by the RCMs, as suggested by Cha et al. (2016). In four RCP simulations for 25 years in the future (2076–2100), precipitation amounts typically increase, especially in summer, compared with

Table 1
Results of sensitivity analysis and calibrated values of dominant parameters, which are closely related with the variability of flow, sediment loads, and fecal coliform bacteria loads.

Parameter	Sensitivity rank	Description	Range of value	Fitted value	SWAT input file
Flow discharge					
Alpha_Bf	1	Baseflow recession constant	0.5–1.0	0.954	.gw
Ch_N2	2	Manning coefficient for channel	0–1	0.029	.rte
Cn2	3	SCS runoff curve number for moisture condition 2	−25-25	0.015	.mgt
Ch_K2	4	Effective hydraulic conductivity in main channel alluvium (mm/h)	−0.01-150	126.0	.rte
Rchrg_dp	5	Deep aquifer percolation fraction	0.0–0.5	0.085	.gw
Sol_Awc	6	Available water capacity of the soil layer (mm/mm soil)	−25-25	−0.375	.sol
Epco	7	Plant uptake compensation factor	0.0–1.0	0.22	.hru
Biomix	8	Biological mixing efficiency	0–1	0.805	.mgt
Slsubbsn	9	Average slope length	10–150	135.0	.hru
Esco	10	Soil evaporation compensation factor	0–1	0.285	.hru
Sediment					
Spcon	1	Coefficient in sediment transport equation	0.0001–0.01	0.003	.bsn
Prf_Bsn	2	Peak rate adjustment factor in the subbasin	0–2	1.206	.bsn
Ch_Cov1	3	Channel bank erodibility factor	−0.05-0.6	0.599	.rte
Ch_Cov2	4	Channel bed erodibility factor	−0.001-1	0.001	.rte
SPEXP	5	Exponent in sediment transport equation	1–1.5	1.006	.bsn
USLE_P	6	USLE support practice factor in the main channel	0.1–1	0.5	.mgt
ADJ_PKR	7	Peak rate adjustment factor	0.0–2.0	1.99	.bsn
Fecal indicator bacteria					
Bsc1	1	The regression coefficients in streambed bacteria concentration equation	0–20	0.77	–
Bsc4	2	The regression coefficients in streambed bacteria concentration equation	0–10	0.94	–
Wgps	3	Growth factor for persistent bacteria adsorbed to soil particles	0–0.5	0.02	.bsn
Wdps	4	Die-off factor for persistent bacteria adsorbed to soil particles	0–0.5	0.25	.bsn
Bact_Swf	5	Fraction of manure applied to land areas that has active colony forming units	0–1	0.2	.bsn
Bactkddb	6	Bacteria partition coefficient in manure	0–1	0.45	Fert.dat

the historical simulation, although inter-model spreads are large. As indicated by Kim et al. (2018) the substantial increase in precipitation during future summer seasons can be associated with increasing convective instability caused by global warming. However, monthly precipitation amount varies according to the four RCP scenarios. In RCP2.6 time series, there are two peaks in June and August, and inter-model discrepancy for monthly precipitation is significantly large from August to October. In RCP4.5, there is one peak in contrast to two peaks in RCP2.6, whereas precipitation changes in RCP6.0 are similar to those in RCP2.6. In RCP8.5, increasing precipitation amount as well as inter-model uncertainty are the largest compared with the other RCP scenarios. In summary, even though precipitation changes are not proportional to changes in radiative forcing, precipitation amount tends to increase during the summer season in all scenarios.

The monthly bias-corrected near-surface mean temperature at Ulsan is shown in Fig. S3. In observations, temperature gradually increases from January, and its maximum of 24.8 °C appears in August. Then, it steadily decreases, with a minimum of about 1.8 °C in January. Variation of monthly average temperature in the historical simulation is similar to the observations, and differences between predictions from different models are relatively small compared with those of precipitation because model dependency for temperature is comparatively small. Under four RCP scenarios, the temperature increment is more significant as radiative forcing increases. Also, temperature tends to increase more in warm seasons than in cold seasons. Similarly to the historical simulation, inter-model uncertainty is relatively small, but is largest in August when the uncertainty of individual model tends to increase substantially due to the future changes in various phenomena such as East Asia summer monsoon, typhoons, and heat waves.

3.3. Impacts of climate change on FCB loads

Fig. S4 shows the projected changes in weather, hydrology, and water quality in response to the 40 bias-corrected GCM-RCM projections for the years 2076 to 2100 as well as current climate conditions for the year 2007 to 2016. The box plots of the individual RCP scenarios were generated from five RCM outputs using two bias correction methods. The projected results were compared with the simulated values using the current climate, which is represented by the black line in the plots of Fig. S4. All RCP scenarios showed remarkable increases in precipitation and temperature compared with the current weather. The RCP 8.5 scenario showed the largest increase in both temperature and precipitation, followed by RCP 6.0, RCP 4.5, and RCP 2.6. Surface runoff also drastically increased under all RCP scenarios in accordance with the increase in precipitation; the surface runoff under the RCP 6.0 scenario was higher than that under RCP 8.5. This difference can be attributed to the rise of evaporation under RCP 8.5 associated with the large temperature difference between RCP 6.0 and RCP 8.5. The increasing patterns of sediment and FCB loads also matched the trend of precipitation. To better understand the influences of precipitation and temperature on FCB, we analyzed all pathways related to the fate and transport of FCB from the input data of varying weather conditions to the simulation output of FCB loads.

Fig. 2 presents the percentage change of hydrology and water quality variables in the watershed according to two scenarios that represent the extreme changes in precipitation and temperature compared with the current climate conditions. We selected RCP2.6_WRF_PT (Scenario I) with large change in precipitation (43.1%) compared with temperature (12.2%) and the RCP8.5_RegCM_QM (Scenario II) scenario with large change in temperature (25.1%) compared with precipitation (8.4%). In terms of the hydrologic response, evaporation caused a large amount of water loss from the watershed (57.4%). Meanwhile, water yield, groundwater flow, lateral flow, and surface runoff were sensitive to changes in precipitation (Fig. 2(a)). In our study area, groundwater flow had the largest percentage of water yield, followed by surface flow and lateral flow.

In Scenario I, it was found that groundwater flow, lateral flow, and surface runoff increased by 69.5%, 40.1%, and 119.0% (Fig. 2(a)), respectively, as compared with the changes caused by Scenario II (19.8%, 5.0%, and 41.7%). Many studies have confirmed that changes in precipitation induce considerable variation of surface runoff (Githui et al. 2009; Hasan et al. 2018; Shen et al. 2017). Increases in surface runoff and

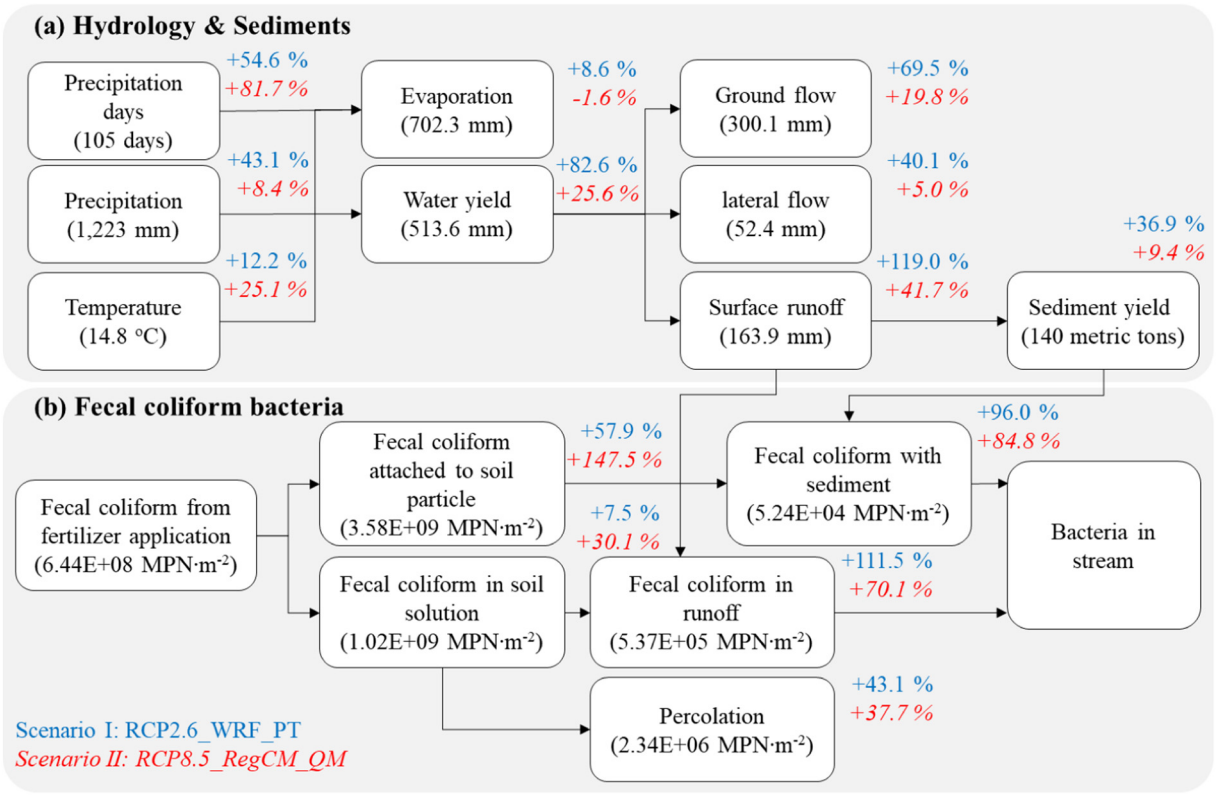

Fig. 2. Flowchart for the estimation of weather input variability and simulated model results in analyzing the impact of climate change on fate and transport of fecal coliform bacteria by selecting the maximum change in precipitation or maximum change in temperature scenarios compared with current climate conditions. Italic font and colors distinguish scenarios I and II. Results for the current climate conditions are within rounded rectangles. The percentage values show he change relative to current climate conditions.

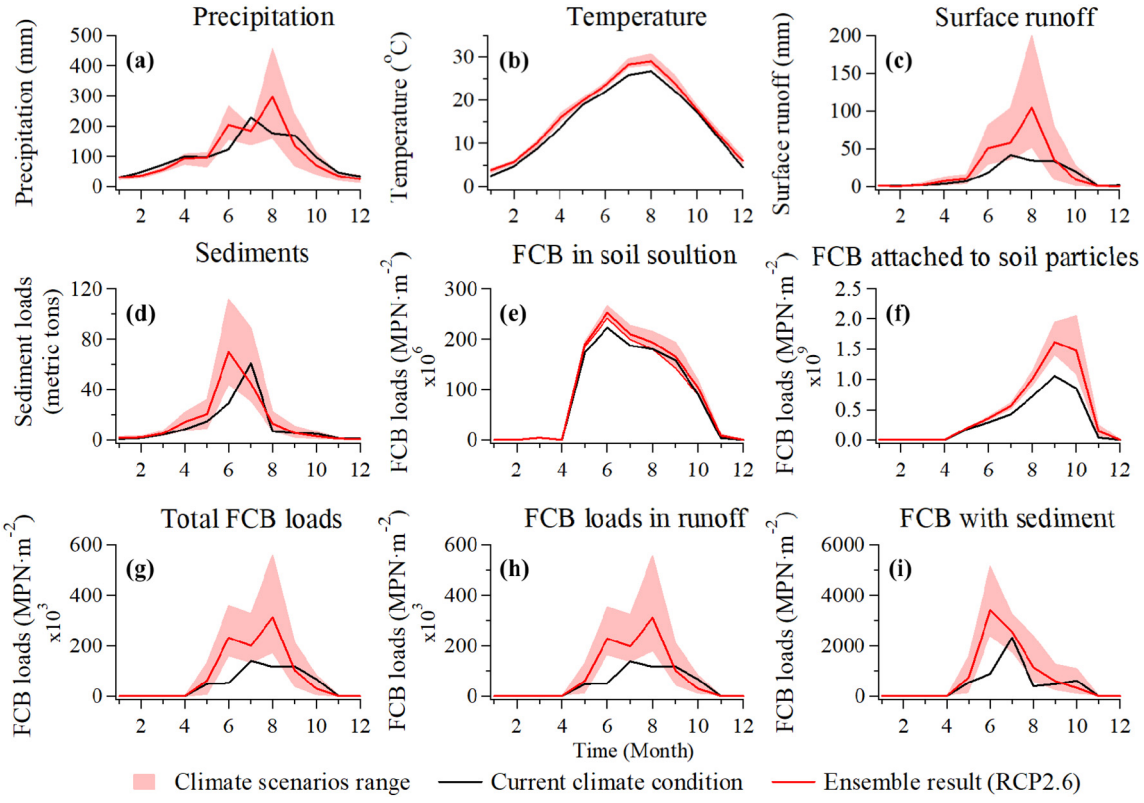

Fig. 3. Comparison of soil simulation results under current climate conditions (2007–2016) and monthly multi-ensemble simulation (MMES) outputs for future climate conditions (2076–2100).

soil erosion lead to increases in sediment loads. We determined that the hydrologic and sediment responses were more sensitive to precipitation level than to temperature. However, the fate and transport of FCB showed close correlation not only with precipitation but also with temperature.

FCB entered the watershed through manure application in the agricultural area shown in the Fig. 2(b) diagram, and became either attached to the soil particles or incorporated in the soil solution based on the bacteria partition coefficient in manure (Bactkddb). The original version of the SWAT model could not simulate re-growth of bacteria in soil. The modified SWAT model simulated the growth by introducing the temperature controls. Medema et al. (1997) found that *E. coli* numbers increased over a two-week period at 15 °C in river water. Bannister (2010) observed that coliform bacteria in soil increased over the seven days and survived over a 28 day period at 20 °C. García-Orenes et al. (2007) discovered that coliforms survived in moist soil at temperatures above 20 °C. Based on the above observations, we considered temperatures ranging from 15 °C to 20 °C for the calibration process. It was determined that 17 °C gave the highest accuracy; therefore, it was chosen as the threshold for bacteria re-growth. When the air temperature is greater than the threshold, soil bacteria start proliferating. Therefore, the amounts of FCB both attached to soil particles and incorporated in soil solution increased during humid and warmer seasons, as shown in Fig. 3. Under Scenario II, FCB rapidly multiplied with increasing temperature on soil particles (147.5%) and in soil solution (30.1%) compared with Scenario I (soil particle: 57.9%; soil solution: 7.5%). Upon entering the stream, FCB loading via sediments and surface runoff increased by over 90% under Scenario I, whereas Scenario II had <90% increase in FCB. It can be concluded that FCB loads in the stream were considerably more sensitive to variations of surface runoff and sediment loads compared with temperature.

The influence of temperature on the survival can be substantially affected by environmental conditions of a specific freshwater body. Protozoa grazing affects coliform populations in water, and for some gazers the maximum activity was found in the range of temperatures 15 °C to 20 °C (McCambridge and McMeekin 1980). Nutrient availability is a key issue in the survival of microbes in soil in water (Jamieson et al., 2002). Organic matter increases the retention of nutrients, provides a carbon source for bacterial species. Coliform growth in presence of organic nutrient source was documented both in soil and in water (Blaustein et al. 2013; Park et al. 2016). Algae can provide both nutrients and physical protection from solar radiation for bacteria including coliforms (Cole 1982; Ansa et al. 2011). Overwetting can have a negative effect on *E. coli* survival due to a lack of usable organic carbon in dilute mixtures (Chandler and Craven 1980). Given the above complexity, the threshold temperature of 17 °C in Eq. 3 appears to be a lumped parameter value of which should be verified for site specific conditions. We hypothesize that in our site-specific conditions growth of FCB cam occur due to the abundance of nutrients due in water and in soil due to manure application in agricultural areas.

3.4. Variation of FCB in the soil under future climate condition

Fig. 3 illustrates the monthly weather inputs and simulation results under current and future climate conditions. From Fig. 3(a) and (b), the precipitation and temperature show clear seasonal patterns with strong peaks during the summer season (June to September), and smaller values in the winter season (November to February). In particular, the summer season at the end of this century showed significant increases in precipitation and temperature. The precipitation increase during the summer season appeared to have a direct influence on surface runoff (Fig. 3(c)). Therefore, the highest peak of surface runoff in July under the current climate conditions was moved to August under future climate condition.

At the start of the year, the average monthly sediment load in Fig. 3 (d) increased and peaked in July (current climate conditions) and in June (future climate conditions), then gradually decreased in the following months. The first reason for the difference of peaks for sediment loads was the increase of surface runoff under the future climate, which occurred one month ahead of the peak for the current climate conditions. Secondly, tillage of rice paddies in May disturbed the soil structure and elevated the erodibility of the soil within the agricultural area (Desta 2000; Guzman et al. 2013). The sediment load consequently decreased with crop growth, even when surface runoff was higher near the end of the summer season (August).

FCB was introduced in the soil of rice paddies by manure application in May. Fig. 3(e) shows the fate and transport of FCB in the soil solution. The bacteria experienced growth in June and survived until October under both climate conditions because of high temperatures during these months despite the bacteria being transported via surface runoff and percolation (Fig. 3(e)). However, it experienced die-off from September to April because of lower temperatures. The FCB attached to soil particles in Fig. 3(f) gradually rises from May to September, compared with the sudden increase of FCB in soil solution shown in Fig. 3 (e). The pattern in Fig. 3(f) clearly shows the re-growth trend of FCB during this period. When estimating the projected change in the amounts of FCB in the soil, the values were higher under the future climate than under the current climate.

Fig. 3(g) presents the monthly total FCB loads in the present and future scenarios. The total FCB load is the summation of the FCB loads in runoff and with sediments, shown in Fig. 3(h) and (i), respectively. The patterns of the monthly total FCB load and the FCB load in runoff were fairly similar to the monthly surface runoff found in Fig. 3(c), Whereas the FCB with sediment was similar to the monthly sediment load in Fig. 3(d). The FCB loads in runoff did not have a substantial difference from the total FCB loads because the amounts of FCB with sediment were negligible (Fig. 3(h)). FCB in soil solution and FCB attached to soil particles were transported via surface runoff as FCB loads in runoff and FCB with sediment, respectively. However, only negligible amounts of FCB with sediment ended up in the water body compared with the original amounts indicated in Fig. 3(f).

FCB loads in runoff contributed greatly to the total FCB loads, which implies that the amount of FCB in soil solution strongly affects the total FCB load. Total FCB loads were remarkably sensitive to changes in precipitation; therefore, the drastic increases of the FCB amounts shown in Fig. 3(g) for future scenarios were expected based on the high precipitation levels in the summer season. From these simulation results, we conclude that reducing FCB in runoff is an effective management strategy rather than reducing FCB with sediment to mitigate total FCB loads. Therefore, increasing infiltration into the soil can be recommended as the most effective management strategy for the TRW among many best management practices (BMPs) (e.g., detention ponds, wetlands, biofiltration, bioretention, and riparian buffers). In field experiments, several BMPs (wetlands and ponds) have low effectiveness in reducing bacteria and in some cases have the potential to export bacteria (Clary et al. 2008).

3.5. Variation of the number of FCB in stream under future climate change

Fig. 4 shows the fate and transport diagram of in-stream FCB under the current climate conditions and future climate scenarios, which includes the percentage changes of FCB loads depending on different weather conditions at the end of this century. The number of FCB in stream were calculated by considering surface runoff from land, resuspension and hyporheic exchange at the streambed, die-off in the stream, and deposition to the streambed. Based on the number of FCB of each process found in Fig. 4, resuspension ($2.92E+13$ MPN·d^{-1}) was determined as the major contributor, followed by surface runoff and hyporheic exchange. In contrast, the deposition process was more influential in decreasing the number of FCB rather than die-off. Scenarios I and II, as defined above, were applied to the in-stream simulations. When we compared the variability of the number of FCB under different

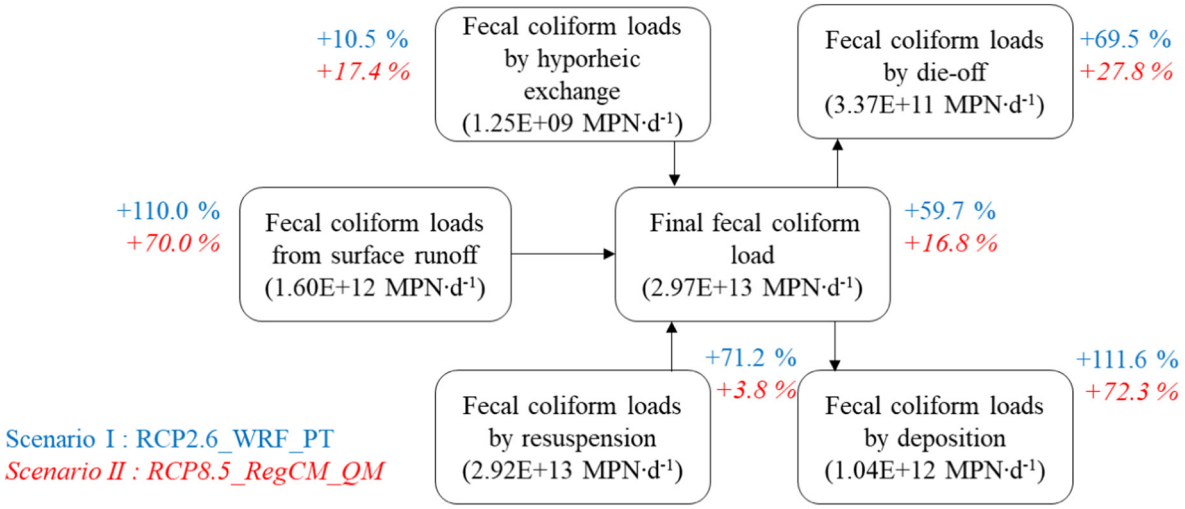

Fig. 4. The variation of fate and transport of FCB in stream according to the largest change in precipitation scenario (Scenario I) and the largest change in temperature scenario (Scenario II) compared with current climate conditions. Results for the current climate conditions are within rounded rectangles. The percentage values show he change relative to current climate conditions.

scenarios, resuspension showed the largest difference in percentage changes in the total number of FCB in Scenario I (71.2%) and Scenario II (3.8%). These changes resulted from the increases in peak channel velocity and volume of water in the reach segment (Neitsch et al. 2011). Therefore, these hydrologic responses, largely caused by precipitation (Scenario I), were more influential in the fate and transport of in-stream FCB as compared with temperature.

Fig. 5 illustrates the monthly variations of the number of FCB in stream under the current climate condition and MMES. Fig. 5(a) and (b) show that the total and resuspended FCB increased under the future climate conditions, especially from June to August. A similar trend in the monthly precipitation shown in Fig. 3(a). Fig. 5(c) presents the monthly die-off of FCB, which shows a similar pattern with the total number of FCB. The amount of FCB die-off increased with the total number of FCB. From Fig. 5(d), the FCB from runoff showed peaks in March, May, and August, which represent manure application periods. The loadings during these months are higher under the future climate scenarios than under the current climate. The amount of deposited FCB to the stream bed in Fig. 5(e) shows similar results with FCB loads from runoff, with peaks in March, May, and August. Fig. 5(f) shows the FCB released into the stream by hyporheic exchange, wherein observable amounts of loading during the dry winter season were also present.

As shown in Fig. 5, the change of the total number of FCB between the future and current climate conditions were similar to resuspension of FCB from the stream bed. Strong correlation between FCB concentration and resuspension from the stream bed was also observed in laboratory and field-based experiments by Abia et al. (2017). Thus, we could deduce that FCB influx from the stream bed should increase in-stream presence of FCB by the end of this century. FCB are used as indicator organisms for the presence of pathogens in stream waters, and FCB concentrations are employed to evaluate microbial water quality for recreation, irrigation and other purposes. Therefore, it is important to know what part the FCB population in water reflects the influx of microbes from the land-based sources where pathogenic organisms can reside along with FCB. It appears that water quality monitoring must be accompanied by stream bed monitoring. Water quality monitoring

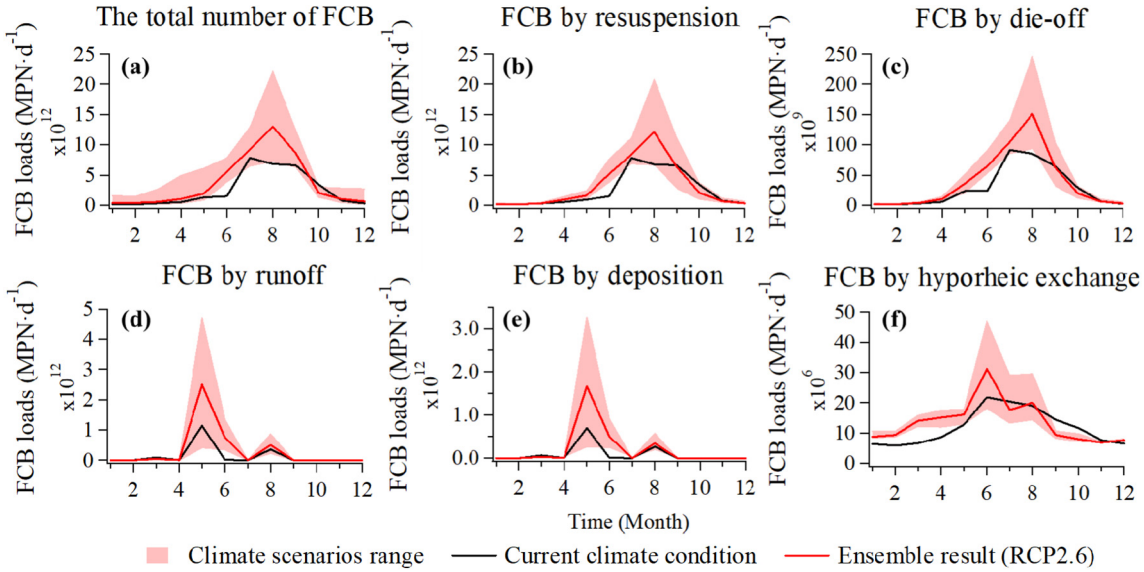

Fig. 5. Simulation results for components of the FCB mass balance at the Taehwa River watershed.

must be accompanied by stream bed monitoring. New monitoring systems may help to better understand the fate and transport of FCB and develop stream management strategies in Korea.

4. Conclusion

This study evaluated the impacts of future climate change on the fate and transport of FCB using MMES and 40 bias-corrected GCM-RCM projections. The original SWAT model yielded a satisfactory performance in calibrating and simulating the current and future seasonal variability of flow and accompanying sediment loads. In addition, the soil and in-stream bacteria modules of the SWAT model were successfully modified by adding descriptions bacteria growth and hyporheic exchange. The prediction accuracy of the seasonal variability of FCB loads was improved, and the sensitivity of FCB based on changes in precipitation and temperature was also verified. The following are the conclusions drawn from this study:

1. For the fate and transport of FCB, the amount of FCB in the soil rapidly increased with increasing temperature. However, precipitation was dominant in transporting FCB from the soil surface to water bodies than temperature. It was also determined that resuspension controlled the final amount FCB concentrations in stream.
2. The multi-model ensemble simulations predicted that FCB originating from soil would drastically increase FCB loads to streams in summer by the end of this century.
3. The monitoring strategies of FCB at the stream bed are essential to evaluate actual and potential microbial water quality in streams

The modified SWAT model can promote understanding of the fate and transport of FCB depending on the variability of weather conditions, and can help to develop an effective strategy to combat microbial contamination of waters in future climate change conditions.

Acknowledgements

This work was supported by Korea Environment Industry & Technology Institute (KEITI) through "The Chemical Accident Prevention Technology Development Project", funded by Korea Ministry of Environment (MOE) (No. 2016001970001).

This research was supported by the Korea Meteorological Administration Research and Development Program under Grant KMI 2018-03310.

Appendix A. Supplementary data

Supplementary data to this article can be found online at https://doi.org/10.1016/j.scitotenv.2018.12.213.

References

Abia, A.L.K., James, C., Ubomba-Jaswa, E., Benteke Momba, M.N., 2017. Microbial remobilisation on riverbed sediment disturbance in experimental flumes and a human-impacted river: implication for water resource management and public health in developing sub-saharan African countries. Int. J. Environ. Res. Public Health 14 (3), 306. https://doi.org/10.3390/ijerph14030306.

Alexander, L., Zhang, X., Peterson, T., Caesar, J., Gleason, B., Klein Tank, A., Haylock, M., Collins, D., Trewin, B., Rahimzadeh, F., 2006. Global observed changes in daily climate extremes of temperature and precipitation. J. Geophys. Res. Atmos. 111 (D5). https://doi.org/10.1029/2005JD006290.

Ansa, E.D.O., Lubberding, H.J., Ampofo, J.A., Gijzen, H.J., 2011. The role of algae in the removal of *Escherichia coli* in a tropical eutrophic lake. Ecol. Eng. 37 (2), 317–324. https://doi.org/10.1016/j.ecoleng.2010.11.023.

Arnold, J.G., Srinivasan, R., Muttiah, R.S., Williams, J.R., 1998. Large area hydrologic modeling and assessment part I: model development. J. Am. Water Resour. Assoc. 34 (1), 73–89. https://doi.org/10.1111/j.1752-1688.1998.tb05961.x.

Baek, H.-J., Lee, J., Lee, H.-S., Hyun, Y.-K., Cho, C., Kwon, W.-T., Marzin, C., Gan, S.-Y., Kim, M.-J., Choi, D.-H., 2013a. Climate change in the 21st century simulated by HadGEM2-AO under representative concentration pathways. Asia-Pac. J. Atmos. Sci. 49 (5), 603–618. https://doi.org/10.1007/s13143-013-0053-7.

Baek, H.J., Lee, J., Lee, H.S., Hyun, Y.K., Cho, C., Kwon, W.T., Marzin, C., Gan, S.Y., Kim, M.J., Choi, D.H., Lee, J., Lee, J., Boo, K.O., Kang, H.S., Byun, Y.H., 2013b. Climate change in the 21st century simulated by HadGEM2-AO under representative concentration pathways. Asia-Pac. J. Atmos. Sci. 49 (5), 603–618. https://doi.org/10.1007/s13143-013-0053-7.

Baffaut, C., Sadeghi, A., 2010. Bacteria modeling with SWAT for assessment and remediation studies: a review. Trans. ASABE 53 (5), 1585–1594.

Bannister, E., 2010. Evaluation of Methodology for Detection and Quantification of Coliform Bacteria and Their Survival in Soil and Water. https://doi.org/10.13031/2013.34907.

Baxter-Potter, W.R., Gilliland, M.W., 1988. Bacterial pollution in runoff from agricultural lands. J. Environ. Qual. 17 (1), 27–34. https://doi.org/10.2134/jeq1988.00472425001700010004x.

Benham, B.L., Baffaut, C., Zeckoski, R.W., Mankin, K.R., Pachepsky, Y.A., Sadeghi, A., Brannan, K.M., Soupir, M., Habersack, M., 2006. Modeling bacteria fate and transport in watersheds to support TMDLs. Trans. ASABE 49 (4), 987–1002. https://doi.org/10.13031/2013.21739.

Blaustein, R.A., Pachepsky, Y., Hill, R.L., Shelton, D.R., Whelan, G., 2013. *Escherichia coli* survival in waters: temperature dependence. Water Res. 47 (2), 569–578. https://doi.org/10.1016/j.watres.2012.10.027.

Cha, S.M., Lee, S.W., Park, Y.E., Cho, K.H., Lee, S., Kim, J.H., 2010. Spatial and temporal variability of fecal indicator bacteria in an urban stream under different meteorological regimes. Water Sci. Technol. 61 (12), 3102–3108. https://doi.org/10.2166/wst.2010.261.

Cha, D.H., Lee, D.K., Jin, C.S., Kim, G., Choi, Y., Suh, M.S., Ahn, J.B., Hong, S.Y., Min, S.K., Park, S.C., Kang, H.S., 2016. Future changes in summer precipitation in regional climate simulations over the Korean Peninsula forced by multi-RCP scenarios of HadGEM2-AO. Asia-Pac. J. Atmos. Sci. 52 (2), 139–149. https://doi.org/10.1007/s13143-016-0015-y.

Chandler, D.S., Craven, J.A., 1980. Relationship of soil moisture to survival of *Escherichia coli* and *Salmonella typhimurium* in soils. Aust. J. Agric. Res. 31 (3), 547–555.

Cho, K.H., Cha, S.M., Kang, J.-H., Lee, S.W., Park, Y., Kim, J.-W., Kim, J.H., 2010. Meteorological effects on the levels of fecal indicator bacteria in an urban stream: a modeling approach. Water Res. 44 (7), 2189–2202. https://doi.org/10.1016/j.watres.2009.12.051.

Cho, K.H., Pachepsky, Y.A., Kim, M., Pyo, J., Park, M.-H., Kim, Y.M., Kim, J.-W., Kim, J.H., 2016a. Modeling seasonal variability of fecal coliform in natural surface waters using the modified SWAT. J. Hydrol. 535, 377–385. https://doi.org/10.1016/j.jhydrol.2016.01.084.

Cho, K.H., Pachepsky, Y.A., Oliver, D.M., Muirhead, R.W., Park, Y., Quilliam, R.S., Shelton, D.R., 2016b. Modeling fate and transport of fecally-derived microorganisms at the watershed scale: state of the science and future opportunities. Water Res. 100, 38–56. https://doi.org/10.1016/j.watres.2016.04.064.

Clary, J., Jones, J., Urbonas, B., Quigley, M., Strecker, E., Wagner, T., 2008. Can stormwater BMPs remove bacteria? New findings from the international stormwater BMP database. Stormwater Mag. May (5), 1–14.

Cole, J.J., 1982. Interactions between bacteria and algae in aquatic ecosystems. Annu. Rev. Ecol. Evol. Syst. 13 (1), 291–314.

Desta, L., 2000. Land Degradation and Strategies for Sustainable Development in the Ethiopian Highlands: Amhara Region. 32. ILRI (aka ILCA and ILRAD).

García-Orenes, F., Roldán, A., Guerrero, C., Mataix-Solera, J., Navarro-Pedreno, J., Gomez, I., Mataix-Beneyto, J., 2007. Effect of irrigation on the survival of total coliforms in three semiarid soils after amendment with sewage sludge. Waste Manag. 27 (12), 1815–1819. https://doi.org/10.1016/j.wasman.2006.08.012.

Gitau, M., Veith, T., Gburek, W., 2004. Farm–level optimization of BMP placement for cost–effective pollution reduction. Trans. ASABE 47 (6), 1923. https://doi.org/10.13031/2013.17805.

Githui, F., Gitau, W., Mutua, F., Bauwens, W., 2009. Climate change impact on SWAT simulated streamflow in western Kenya. Int. J. Climatol. 29 (12), 1823–1834. https://doi.org/10.1002/joc.1828.

Graczyk, T.K., Sunderland, D., Awantang, G.N., Mashinski, Y., Lucy, F.E., Graczyk, Z., Chomicz, L., Breysse, P.N., 2010. Relationships among bather density, levels of human waterborne pathogens, and fecal coliform counts in marine recreational beach water. Parasitol. Res. 106 (5), 1103–1108. https://doi.org/10.1007/s00436-010-1769-2.

Grant, S.B., Litton-Mueller, R.M., Ahn, J.H., 2011. Measuring and modeling the flux of fecal bacteria across the sediment-water interface in a turbulent stream. Water Resour. Res. 47 (5). https://doi.org/10.1029/2010WR009460.

Guan, T.Y., Holley, R.A., 2003. Pathogen survival in swine manure environments and transmission of human enteric illness—a review. J. Environ. Qual. 32 (2), 383–392. https://doi.org/10.2134/jeq2003.3830.

Guzman, C., Tilahun, S., Zegeye, A., Steenhuis, T., 2013. Suspended sediment concentration-discharge relationships in the (sub-) humid Ethiopian highlands. Hydrol. Earth Syst. Sci. 17 (3), 1067. https://doi.org/10.5194/hess-17-1067-2013.

Hagedorn, C., Robinson, S.L., Filtz, J.R., Grubbs, S.M., Angier, T.A., Reneau, R.B., 1999. Determining sources of fecal pollution in a rural Virginia watershed with antibiotic resistance patterns in fecal *streptococci*. Appl. Environ. Microbiol. 65 (12), 5522–5531.

Hargreaves, G.L., Hargreaves, G.H., Riley, J.P., 1985. Agricultural benefits for Senegal River basin. J. Irrig. Drain. Eng. 111 (2), 113–124. https://doi.org/10.1061/(ASCE)0733-9437(1985)111:2(113).

Hasan, E., Tarhule, A., Kirstetter, P.-E., Clark III, R., Hong, Y., 2018. Runoff sensitivity to climate change in the Nile River basin. J. Hydrol. 561, 312–321. https://doi.org/10.1016/j.jhydrol.2018.04.004.

Hendricks, C.W., 1972. Enteric bacterial growth rates in river water. Appl. Microbiol. 24 (2), 168–174.

Hofstra, N., 2011. Quantifying the impact of climate change on enteric waterborne pathogen concentrations in surface water. Curr. Opin. Environ. Sustain. 3 (6), 471–479. https://doi.org/10.1016/j.cosust.2011.10.006.

Hong, H., Qiu, J., Liang, Y., 2010. Environmental factors influencing the distribution of total and fecal coliform bacteria in six water storage reservoirs in the Pearl River Delta Region, China. J. Environ. Sci. 22 (5), 663–668. https://doi.org/10.1016/S1001-0742(09)60160-1.

Jamieson, R.C., Gordon, R.J., Sharples, K.E., Stratton, G.W., Madani, A., 2002. Movement and persistence of fecal bacteria in agricultural soils and subsurface drainage water: a review. Can. Biosyst. Eng. 44 (1), 1–9.

Jamieson, R., Gordon, R., Joy, D., Lee, H., 2004. Assessing microbial pollution of rural surface waters: a review of current watershed scale modeling approaches. Agric. Water Manag. 70 (1), 1–17. https://doi.org/10.1016/j.agwat.2004.05.006.

Jeon, D.J., Ki, S.J., Cha, Y., Park, Y., Kim, J.H., 2018. New methodology of evaluation of best management practices performances for an agricultural watershed according to the climate change scenarios: a hybrid use of deterministic and decision support models. Ecol. Eng. 119, 73–83. https://doi.org/10.1016/j.ecoleng.2018.05.006.

Jones, A., Haywood, J.M., Jones, C.D., 2018. Can reducing black carbon and methane below RCP2. 6 levels keep global warming below 1.5 °C? Atmos. Sci. Lett. https://doi.org/10.1002/asl.821.

Kim, M., Boithias, L., Cho, K.H., Silvera, N., Thammahacksa, C., Latsachack, K., Rochelle-Newall, E., Sengtaheuanghoung, O., Pierret, A., Pachepsky, Y.A., 2017. Hydrological modeling of fecal indicator bacteria in a tropical mountain catchment. Water Res. 119, 102–113. https://doi.org/10.1016/j.watres.2017.04.038.

Kim, G., Cha, D.H., Park, C., Lee, G., Jin, C.S., Lee, D.K., Suh, M.S., Ahn, J.B., Min, S.K., Hong, S.Y., Kang, H.S., 2018. Future changes in extreme precipitation indices over Korea. Int. J. Climatol. 38, E862–E874. https://doi.org/10.1002/joc.5414.

Kistemann, T., Claßen, T., Koch, C., Dangendorf, F., Fischeder, R., Gebel, J., Vacata, V., Exner, M., 2002. Microbial load of drinking water reservoir tributaries during extreme rainfall and runoff. Appl. Environ. Microbiol. 68 (5), 2188–2197. https://doi.org/10.1128/AEM.68.5.2188-2197.2002.

Lee, J.-W., Hong, S.-Y., Chang, E.-C., Suh, M.-S., Kang, H.-S., 2014. Assessment of future climate change over East Asia due to the RCP scenarios downscaled by GRIMs-RMP. Clim. Dyn. 42 (3–4), 733–747. https://doi.org/10.1007/s00382-013-1841-6.

Li, Z., Liu, W.-z., Zhang, X.-c., Zheng, F.-l., 2009. Impacts of land use change and climate variability on hydrology in an agricultural catchment on the Loess Plateau of China. J. Hydrol. 377 (1–2), 35–42. https://doi.org/10.1016/j.jhydrol.2009.08.007.

Ligaray, M., Baek, S.S., Kwon, H.-O., Choi, S.-D., Cho, K.H., 2016. Watershed-scale modeling on the fate and transport of polycyclic aromatic hydrocarbons (PAHs). J. Hazard. Mater. 320, 442–457. https://doi.org/10.1016/j.jhazmat.2016.08.063.

Lipp, E.K., Farrah, S.A., Rose, J.B., 2001. Assessment and impact of microbial fecal pollution and human enteric pathogens in a coastal community. Mar. Pollut. Bull. 42 (4), 286–293. https://doi.org/10.1016/S0025-326X(00)00152-1.

Martin, G.M., Bellouin, N., Collins, W.J., Culverwell, I.D., Halloran, P.R., Hardiman, S.C., Hinton, T.J., Jones, C.D., McDonald, R.E., McLaren, A.J., O'Connor, F.M., Roberts, M.J., Rodriguez, J.M., Woodward, S., Best, M.J., Brooks, M.E., Brown, A.R., Butchart, N., Dearden, C., Derbyshire, S.H., Dharssi, I., Doutriaux-Boucher, M., Edwards, J.M., Falloon, P.D., Gedney, N., Gray, L.J., Hewitt, H.T., Hobson, M., Huddleston, M.R., Hughes, J., Ineson, S., Ingram, W.J., James, P.M., Johns, T.C., Johnson, C.E., Jones, A., Jones, C.P., Joshi, M.M., Keen, A.B., Liddicoat, S., Lock, A.P., Maidens, A.V., Manners, J.C., Milton, S.F., Rae, J.G.L., Ridley, J.K., Sellar, A., Senior, C.A., Totterdell, I.J., Verhoef, A., Vidale, P.L., 2011. The HadGEM2 family of met Office unified model climate configurations. Geosci. Model Dev. 4 (3), 723–757. https://doi.org/10.5194/gmd-4-723-2011.

McCambridge, J., McMeekin, T.A., 1980. Relative effects of bacterial and protozoan predators on survival of *Escherichia coli* in estuarine water samples. Appl. Environ. Microbiol. 40 (5), 907–911.

Medema, G., Bahar, M., Schets, F., 1997. Survival of *Cryptosporidium parvum*, *Escherichia coli*, faecal *Enterococci* and *Clostridium perfringens* in river water: influence of temperature and autochthonous microorganisms. Water Sci. Technol. 35 (11−12), 249–252. https://doi.org/10.1016/S0273-1223(97)00267-9.

Meehl, G.A., Arblaster, J.M., Tebaldi, C., 2005. Understanding future patterns of increased precipitation intensity in climate model simulations. Geophys. Res. Lett. 32 (18). https://doi.org/10.1029/2005GL023680.

Moriasi, D.N., Arnold, J.G., Van Liew, M.W., Bingner, R.L., Harmel, R.D., Veith, T.L., 2007. Model evaluation guidelines for systematic quantification of accuracy in watershed simulations. Trans. ASABE 50 (3), 885–900. https://doi.org/10.13031/2013.23153.

Neitsch, S.L., Arnold, J.G., Kiniry, J.R., Williams, J.R., 2011. Soil and Water Assessment Tool Theoretical Documentation Version 2009. Texas Water Resources Institute.

Noor, R., Islam, Z., Munshi, S., Rahman, F., 2013. Influence of temperature on *Escherichia coli* growth in different culture media. J. Pure Appl. Microbiol. 7 (2), 899–904.

Park, Y., Pachepsky, Y., Shelton, D., Jeong, J., Whelan, G., 2016. Survival of manure-borne *Escherichia coli* and fecal coliforms in soil: temperature dependence as affected by site-specific factors. J. Environ. Qual. 45 (3), 949–957. https://doi.org/10.2134/jeq2015.08.0427.

Park, Y., Pachepsky, Y., Hong, E.-M., Shelton, D., Coppock, C., 2017. *Escherichia coli* release from streambed to water column during baseflow periods: a modeling study. J. Environ. Qual. 46 (1), 219–226. https://doi.org/10.2134/jeq2016.03.0114.

Schär, C., Lüthi, D., Beyerle, U., Heise, E., 1999. The soil–precipitation feedback: a process study with a regional climate model. J. Clim. 12 (3), 722–741. https://doi.org/10.1175/1520-0442(1999)012<0722:TSPFAP>2.0.CO;2.

Scott, T.M., Rose, J.B., Jenkins, T.M., Farrah, S.R., Lukasik, J., 2002. Microbial source tracking: current methodology and future directions. Appl. Environ. Microbiol. 68 (12), 5796–5803. https://doi.org/10.1128/AEM.68.12.5796-5803.2002.

Shen, Q., Cong, Z., Lei, H., 2017. Evaluating the impact of climate and underlying surface change on runoff within the Budyko framework: a study across 224 catchments in China. J. Hydrol. 554, 251–262. https://doi.org/10.1016/j.jhydrol.2017.09.023.

Sinton, L.W., Hall, C.H., Lynch, P.A., Davies-Colley, R.J., 2002. Sunlight inactivation of fecal indicator bacteria and bacteriophages from waste stabilization pond effluent in fresh and saline waters. Appl. Environ. Microbiol. 68 (3), 1122–1131. https://doi.org/10.1128/AEM.68.3.1122-1131.2002.

Sinton, L.W., Braithwaite, R.R., Hall, C.H., Mackenzie, M.L., 2007. Survival of indicator and pathogenic bacteria in bovine feces on pasture. Appl. Environ. Microbiol. 3 (24), 7917–7925. https://doi.org/10.1128/AEM.01620-07.

St Laurent, J., Mazumder, A., 2014. Influence of seasonal and inter-annual hydrometeorological variability on surface water fecal coliform concentration under varying land-use composition. Water Res. 48, 170–178. https://doi.org/10.1016/j.watres.2013.09.031.

Teutschbein, C., Seibert, J., 2012. Bias correction of regional climate model simulations for hydrological climate-change impact studies: review and evaluation of different methods. J. Hydrol. 456, 12–29. https://doi.org/10.1016/j.jhydrol.2012.05.052.

Trenberth, K.E., 2011. Changes in precipitation with climate change. Clim. Res. 47 (1/2), 123–138. https://doi.org/10.3354/cr00953.

Wentz, F.J., Ricciardulli, L., Hilburn, K., Mears, C., 2007. How much more rain will global warming bring? Science 317 (5835), 233–235. https://doi.org/10.1126/science.1140746.

Whitman, R.L., Nevers, M.B., Korinek, G.C., Byappanahalli, M.N., 2004. Solar and temporal effects on *Escherichia coli* concentration at a Lake Michigan swimming beach. Appl. Environ. Microbiol. 70 (7), 4276–4285. https://doi.org/10.1128/AEM.70.7.4276-4285.2004.